Analysis of post-processing influence on the geometrical and dimensional accuracy of Selective Laser Melting parts

Abstract

Purpose – This work analyses the effect of the different common post-processes on the geometrical and dimensional accuracy of SLM parts.

Design/methodology/approach – An artefact has been designed including cubic features formed by planar surfaces orientated according to the machine axes, covering all the X-Y area of the working space. The artefact has been analysed both geometrically (flatness, parallelism) and dimensionally (sizes, distances) from CMM measurement results at three stages: 1 – as built, 2 – after sand-blasting, and 3 – after stress-relieving heat treatment.

Findings – Results from the SLM machine used in this work lead to smaller parts than the nominal ones. This effect depends on the direction of the evaluated dimension of the parts, i.e. X, Y or Z direction, and is differently affected by the sandblasting post-process (average erosion ratio of 68 μm, 54 μm and 9 μm, respectively), being practically unaltered by the HT applied after.

Originality/value – This paper shows the influence, from a geometric and dimensional point of view, of two of the most common post-processes used after producing SLM parts, such as sand-blasting and stress-relieving heat treatment, that have not been considered in previous research.

Keywords

Additive Manufacturing; Selective Laser Melting; 17-4PH stainless steel; Accuracy; Sandblasting; Stress relieving heat treatment.

1. Introduction

Selective Laser Melting (SLM) is an Additive Manufacturing (AM) technique that permits to produce high-complex fully functional metallic parts. To achieve this, this AM technique results of great interest for several leading sectors such as aerospace, automotive, or medical, in which the dimensional accuracy of the manufactured parts stands out as an important issue.

SLM process belongs to the group classified as Powder Bed Fusion (PBF) techniques, in which a high-density laser selectively melts a thin powder layer distributed upon a built-up plate or upon a previous manufactured layer. During this manufacturing process, the built portion of the part is subjected to a complex thermal cycle which produces residual stresses on the SLM manufactured part, affecting negatively its dimensional accuracy (Matsumoto *et al.*, 2002) as is well known. These deformations can be related to the characteristic AM built-up process itself, but also to SLM laser scanning process parameters (Cheng *et al.*, 2016). According to Bartlett and Li (2019) stated in their analysis of the current state of knowledge, the main parameters of the SLM process that have a major influence upon residual stresses, regardless of the material, are built-up plate heating, laser power, scanning speed and scanning strategy. Apart from other sources of dimensional errors, such as laser spot positioning errors over the powder bed, the deformation induced in the parts by the thermal stresses cited above is still an important issue nowadays. Moreover, all the post-process procedures that can relieve or alter them, i.e., Heat Treatment (HT) post-processes, have to be considered.

Due to the characteristics of the SLM technique and the as-built condition of the parts, several post-processing operations are required. Some of them are mandatory while others permit to improve the quality of the parts, i.e., mechanical properties, dimensional

accuracy, surface quality, etc. This post-processing procedures can be classified as mechanical and HT procedures.

- Mechanical procedures: one of the essentially mandatory mechanical process that has to be carried out in SLM is to separate manufactured parts from the built-up plate. For this purpose, several mechanical processes can be applied, among which the Wire Electrical Discharge Machining (Wire EDM) stands out. In addition, with the aim to improve various quality aspects of the parts (Lesyk *et al.*, 2020), other mechanical post-processes can be applied, such as dry mechanical-electromechanical (Bai *et al.*, 2020), tumbling finishing (Morton *et al.*, 2012), ultrasonic excitation (Tilita *et al.*, 2017), surface rolling (Wang *et al.*, 2017), both external (Avanzini *et al.*, 2019) and internal (Han *et al.*, 2020) abrasive processes, laser polishing (Basha *et al.*, 2020) and different peening processes as laser peening (Hackel *et al.*, 2018), ultrasonic peening (Gale and Achuhan, 2017), shot-peening (AlMangour *et al.*, 2016). Overall, this improvement is aimed at achieving a better surface finish not attainable in the as-built state. The usual processes are sandblasting and shot peening, used in the entire or in local regions of the parts, respectively.

  On the other hand, in order to assemble SLM parts to other parts thus ensuring the interchangeability principle, other processes, such as machining or grinding, are used.

- Heat Treatment procedures: permit to relieve the thermal stresses generated during the SLM process and, depending on the material used, to improve the mechanical properties and to reduce the internal porosity of the parts (Zang *et al.,* 2019), being Hot Isostatic Pressing a high-suited process to achieve them, which can be applied alone (Liu and Guo, 2020) or in combination with homogenization

heat treatment (Mostafa *et al.*, 2017), and which permits compete SLM parts with other powder metallurgy techniques as near-net-shape parts (Kaplanskii *et al.*, 2019).

To date, several research works have studied the metrological characterization of SLM parts, starting from researchers that propose methodologies for modelling the process using dimensionless parameters (van Elsen *et al.*, 2008) to other researchers that focus their work on the surface topography (Senin *et al.*, 2017), or on the dimensional quality (Kalms *et al.*, 2019).

In this approach, Townsend *et al.* (2018) propose a series of three tailor-made measurement test artefacts designed to be used in the verification of AM manufacturing processes. Moreover, other studies analyse the best part orientation during the manufacturing process to achieve the design dimensional specifications with the less post-processing as possible (Das *et al.*, 2015).

As far as the surface quality of the components is concerned, one of the main limitations for its characterization is the absence of standardization. Some researchers as Koutiri *et al.* (2018), focus their work on the influence of different process parameters upon the part surface quality, analysing both the fabricating characteristics of non-support overhanging structure and also the dimensional accuracy by laser scanning of a specific product (Yang *et al.*, 2012). Moreover, others analyse this influence in the fatigue performance, achieving important improvements by means of additional manufacturing processes as milling, blasting and polishing (Bagehorn *et al.*, 2015). In this way, Bagherifard *et al.* (2018) stated that the application of different fast and simple mechanical post-processing as shot-peening and sandblasting, as well as other suitable HTs, can improve substantially the mechanical performance of parts subjected to dynamic loads. Moreover, other

researchers (Ginestra *et al.*, 2020) have proved that these post-processing techniques allow for enhancing the applicability of AM parts to specific medical applications.

Nevertheless, most of these studies focused on part quality usually obviate the importance of various specific aspects related to both the process and post-process of the SLM manufactured parts:

- Almost all PBF techniques use a mechanical device, such as a paddle or roller, to perform the dosage, and in some cases, compaction of the powder upon the bed. This device can act over the powder bed from different directions and following different movement strategies. Moreover, it can apply a different compaction force as required.
- A post-processing procedure that is highly recommended by the manufacturers of PBF machines for the additive manufacturing of metallic parts is a stress-relieving HT, which permits to improve the stability of the material and also the dimensional accuracy of parts.

Considering these SLM specific factors, this research analyses the geometrical and dimensional accuracy of the manufactured parts regarding to:

- Both the positional and dimensional error committed by the SLM machine in the three coordinate axes during the process, i.e., in the roller movement direction (X axis), in the horizontal direction perpendicular to the roller movement (Y axis), and in the height direction (Z axis).
- The effect of sandblasting application as post-processing in order to improve the surface quality of the parts.
- The influence of stress relieving HT to relieve thermal residual stresses and improve mechanical properties of the parts.

In spite of that the first of the effects mentioned above has been studied very recently by the authors of this work (Cuesta *et al.*, 2019), the research has been now extended to analyse the influence of sandblasting and subsequent HT. The influence of these two post-processes with regard to the part dimensional and geometrical quality has not been analysed up to date. This work was carried out using a 17-4PH stainless steel as raw material as it is a high-spread material for this kind of AM process.

2. Material and methods

A metal 3DSystems SLM ProX 100 machine (3DSystems, 2017) has been used to manufacture the specimen part. This SLM machine is equipped with a fibre laser of 1070 nm of wavelength capable to supply a maximum power of 50 W. During the manufacturing process, the manufacturing chamber of the machine was inertized with Nitrogen obtained from a generator connected to it. The maximum manufacturing volume is 100 mm ×100 mm ×100 mm with the same repeatability in the three axes of 20 µm and a typical accuracy of ±0.1-0.2% (±50 µm minimum). In this machine, the metallic powder dosage over the bed is carried out by means of a mechanical roller that moves along the machine *X* axis. This roller executes a movement strategy moving back and forth twice in order to assure a good powder compaction for each layer. Layer thickness can be set between 10 and 30 µm. The SLM ProX 100 machine is capable of manufacturing parts from various metallic alloys. In this work, 17-4PH stainless steel supplied by 3DSystems was used as raw material due to the high-spread use of this alloy in leading sectors such as aerospace industry. Its weight composition is shown in Table I. This precipitation hardened stainless steel maintains great mechanical properties and corrosion resistance up to services temperatures of 300 ºC. In the “as-built” condition of SLM manufactured

parts, this material has a yield strength of 620±30 MPa, being able to reach up it to 1100±50 MPa after a proper HT post-process which promotes the precipitation hardening.

Table I. 3DSystems 17-4PH weight composition specifications.

Element	Fe	Cr	Ni	Cu	Si	Mn	Nb
Weight (%)	Balance	15-17.5	3-5	3-5	< 1.0	< 1.0	0.15-0.45

Values for the main SLM parameters of the machine were tuned based on previous work experiments (Zapico *et al.*, 2018) in order to obtain a laser energy density of 129 J/mm^3, by means of 38 W of laser power, 140 mm/s of scanning speed, 70 μm of hatch distance and 30 μm of layer thickness.

According to Mower and Long (2016) and to the machine manufacturer, SLM manufactured parts must be submitted to a stress relieving HT post-process before being separated from the built-up plate. The purpose is to relieve thermal residual stresses induced during the SLM manufacturing process thus avoiding undesirable geometrical distortions of the parts. The stress relieving HT also produces an increase in the material hardness with respect to the as-built condition, as it was studied in a previous work (Giganto *et al.*, 2019). For this material and this part size, the stress relieving HT recommended by the machine manufacturer involves heating at 650 °C for 2 hours followed by air cooling until reaching the room temperature.

Regarding the post-processes applied in this work, parts were first sandblasted using a Sablex S-2 machine which propels abrasive powder of white aluminium oxide WFA F100 (particles sieved by a 125 μm opening size mesh) at a working pressure of 7 bar through a 4 mm diameter nozzle. The use of this machine is manual, being recommended to maintain a 30 mm distance between the nozzle and the blasted surface for about 4 seconds.

On the other hand, the HT was carried out using a Hobersal 12 PR/400 electric muffle furnace with a maximum temperature of 1200 ºC and regulation of ±1 ºC.

In order to evaluate the geometrical and dimensional accuracy of the specimen described in sub-section 2.1, a Coordinate Measuring Machine (CMM) DEA Global Image equipped with a contact scanning touch-probe Renishaw® SP25 and a 1 mm diameter tip was used. According to ISO 10360-2, its Maximum Permissible Error is given by $MPE_E = 2.1 + 0.003 \cdot L\ [\mu m], L$ being in mm . With the aim of obtaining reliable measurements results, several recommended measurement procedures were carried out, i.e., various repetitions of the measurement program were executed, and the specimen was placed at different orientations in different locations of the CMM working volume.

2.1. Test specimen

In order to relate the dimensional and geometrical manufacturing accuracy of the machine working volume and its powder bed with its cartesian coordinate reference system, a specimen was manufactured which consists of 21 cubes homogenously distributed following a regular matrix in X, Y machine axes (Figure 1a).

Figure 1 (a) Cubes codification based on machine axes (b) CMM measurement of the test part

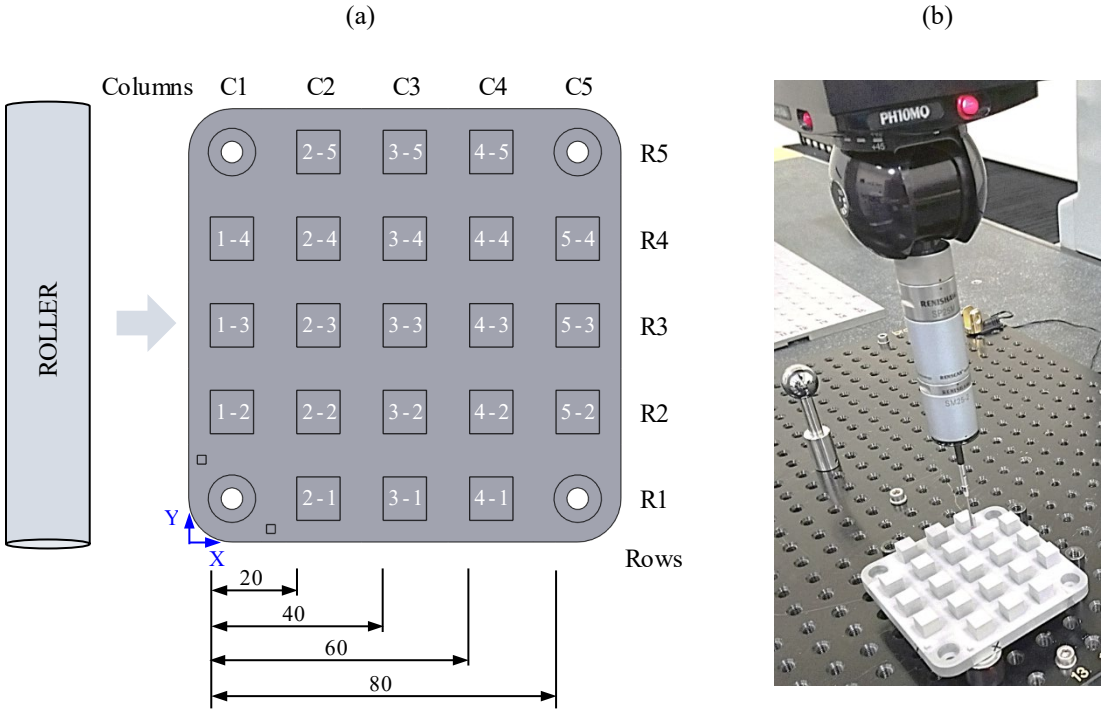

These cubes of the specimen have a nominal dimension of 10 mm × 10 mm with a height of 9.99 mm in order to minimize the dimensional error caused by the slicer software according to the layer thickness used as commented above. The distribution of cubes over the built-up plate was arranged according to a *XY* regular matrix with 10 mm of distance between cubes in both axes, excepting for the corners of the plate where cubes were removed to avoid interfering with the location of the holes required to clamp the plate to the machine table during the SLM process. This kind of geometry, apart from allowing a fast CMM dimensional evaluation (Figure 1b), permits to relate the dimensional and geometrical accuracy of each cube in the specimen with its location over the powder bed surface, i.e., upon the built-up plate. Furthermore, this accuracy can be related to the orientation of the compaction roller and its direction of movement. The different compaction capability of the roller along its movement direction and along its axis direction, i.e. respectively *X* and *Y* axes, could be an important issue in the accuracy

reliability of the manufactured parts. Moreover, all this position/accuracy relation can be applied to the vertical direction by analysing the actual height of the cubes.

2.2. Experimental methodology

In order to analyse the dimensional and geometrical accuracy of the specimen and the possible influence of the sandblasting and stress relieving HT post-processes, the specimen was studied in three conditions:

- As-built condition (AB): the metrological analysis of the specimen in this condition permits to determine the geometrical accuracy of the SLM parts without any kind of post-processing. Furthermore, using this condition as reference, this metrological analysis permits to evaluate the possible variation of the accuracy obtained after performing different post-processing.
- Post sandblasting condition (SB): comparing the analysis of the specimen in this condition with regard to the AB condition allows to determine the possible advantage of using this common post-process for this kind of parts.
- Post sandblasting and subsequent stress relieving HT condition (SB-HT): comparing the analysis in this condition with the previous ones allows to determine the possible effect of the relieving suffered by the specimen on their dimensional accuracy and the advantage of the sequential application of sandblasting and stress-relieving HT post-processes. The stress-relieving HT applied to the specimen was the recommended one by the manufacturer of the SLM machine, that is, heating at 650 °C for 2 hours and air cooling at room temperature.

The metrological analysis for each of the conditions cited above was carried out from CMM measurements so that three measurement result datasets were obtained for the

specimen in the different conditions, i.e. AB, SB, SB-HT. This procedure is schematically represented in Figure 2.

Figure 2 Procedure and conditions of the specimen

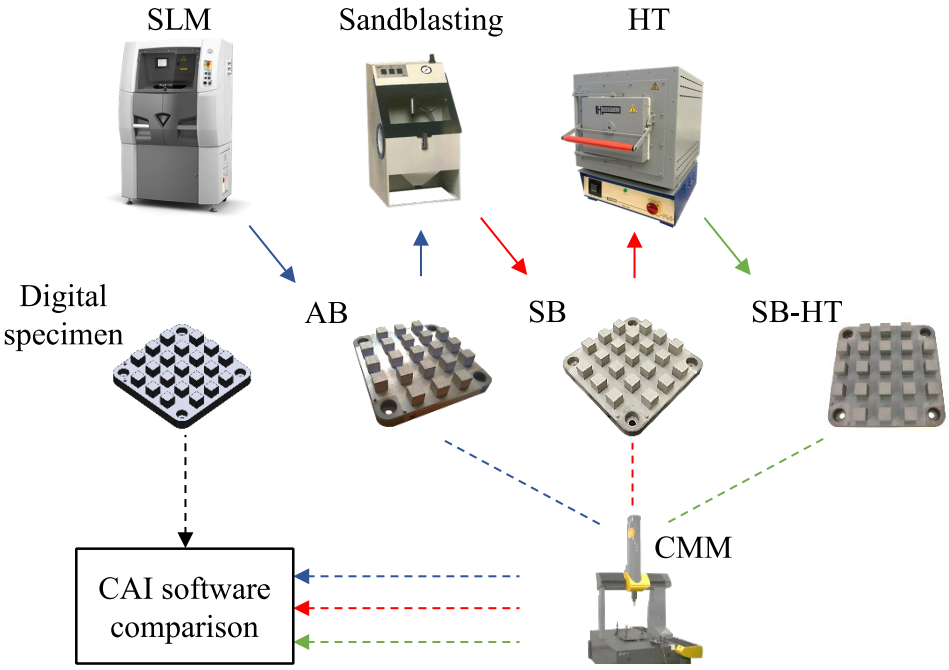

For all these measurements, the five accessible faces of the specimen cubes were measured by probing 100 points in a 10×10 grid on each face. All these digitised data were processed using the Computer Aided Inspection (CAI) software PC-DMIS 2015. For each cube face, a substitute planar entity was reconstructed from the set of digitised points by applying a Least Squares fitting algorithm. Afterwards, the metrological definition of those planar entities, i.e., centroid position and normal vector, were computed. Furthermore, the set of digitised points was also used for determining the form deviation (flatness) of the corresponding cube face.

All this information was utilized later using the same CAI software to evaluate both geometrical and dimensional quality of the specimen.

The evaluation of the geometrical quality involves the analysis of flatness of each planar face of the cubes. In the case of XZ and YZ planes, the average values of flatness of these vertical faces for each cube were considered. Moreover, the parallelism of the top face of the cubes and the build-up plate was also evaluated.

Regarding the dimensional evaluation, two different analyses were carried out. First, deviations of the three size dimensions, i.e., length, width and height, of each cube were considered. Secondly, the distances between homologous faces of different cubes along the X (columns) and Y (rows) directions were measured and compared to their nominal values. In any row/column, the cube face closest to the origin (Figure 1a) was taken as the origin for measuring the respective distances within the respective row/column. As there are no cubes in the specimen corners, the nominal values of the considered distances were 20 mm and 40 mm for the first and fifth rows/columns, and 20 mm, 40 mm, 60 mm and 80 mm for the second, third, and fourth rows/columns.

3. Results and discussion

3.1. Geometrical analysis

The distribution of the measured flatness of all the accessible cubes faces in the three analysed stages are shown in Figure 3. Observing the measured flatness for the AB condition, it can be noticed that, in the case of XZ and YZ faces of the cubes (cubes lateral faces), there is not a remarkable trend related to the cube location along the X and Y axes upon the plate, i.e., flatness quality in case of these cubes faces looks randomly distributed upon the plate. On the contrary, the flatness for the XY planes is influenced for its position in the plate, as the cubes located closer to the origin have worse flatness than those located in the opposite corner of the plate. This X and Y trend can be related to differences in the

compaction capability of the roller, along its movement direction and along its length, respectively.

Figure 3 Distribution of the XZ, YZ, XY cubes faces flatness upon the built-up plate for all conditions. X and Y values refer to location of cube faces within the build plate while "F" values indicate the measured flatness of each cube face.

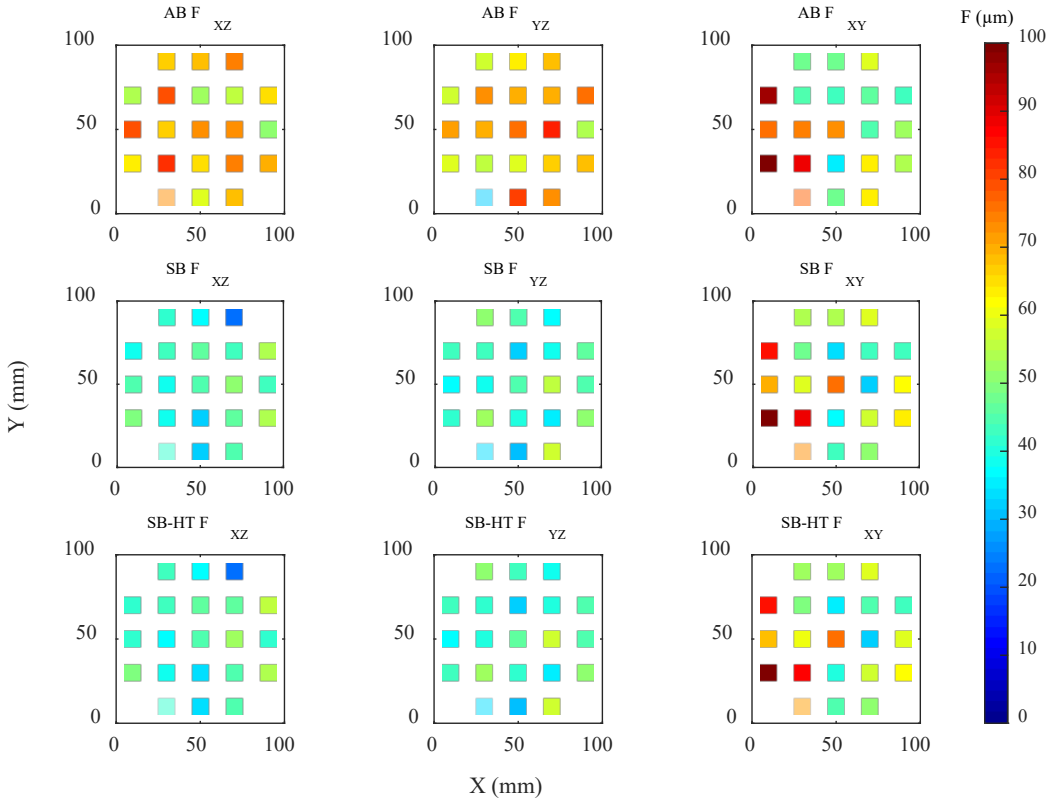

Table II shows the average flatness value of the different cube faces and their standard deviations for all the conditions analysed. In AB condition and in case of vertical cubes faces, it can be noticed that XZ planes flatness is slightly worse than YZ planes flatness. This can be related to the different capability of the roller to compact the powder and, therefore, to the different quantity of projections that are formed during the SLM process and finally are attached to the vertical faces of the parts. An important improvement of the flatness is achieved in case of XZ and YZ faces by means of sandblasting post-process, reducing the mean flatness for both XZ and YZ planes. Flatness of XZ planes is reduced in average from 67.2 µm to 42.1 µm, whereas flatness of YZ planes is reduced in average

from 65.5 µm to 43.1 µm, which supposes a reduction of 25 µm and 23 µm, respectively. Furthermore, the differences observed in the flatness of XZ and YZ faces disappear after sandblasting the specimen. In the case of horizontal cubes faces, i.e., top faces, their flatness is barely modified by the sandblasting process, reaching a slight improvement of 2 µm. To summarize the sandblasting improvement, the percentage of flatness improvement ratio with regard to AB condition is represented in Figure 4. An average flatness improvement ratio of 37.4 %, 35.0 % and 3.8 % is achieved in XZ, YZ and XY cubes faces, respectively.

Table II Flatness of XZ, YZ, XY cubes faces in all conditions analysed

Condition	Flatness (µm)					
	$\overline{F_{XZ}}$	$\sigma_{F_{XZ}}$	$\overline{F_{YZ}}$	$\sigma_{F_{YZ}}$	$\overline{F_{XY}}$	$\sigma_{F_{XY}}$
AB	67.2	9.1	65.5	11.4	60.9	19.1
SB	42.1	7.7	42.6	7.6	58.6	18.7
SB-HT	42.6	7.4	43.1	7.5	58.5	18.1

Figure 4 Sandblasting post-process flatness improvement ratio from as-built condition

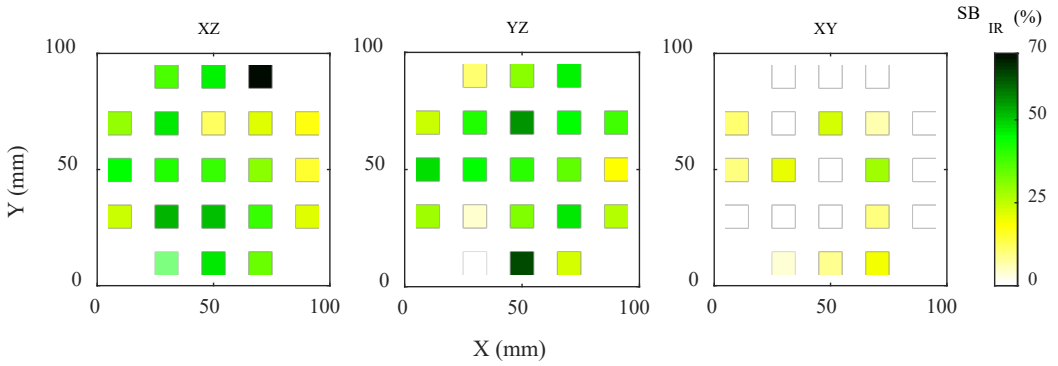

On the other hand, the obtained results do not show significant changes in flatness of both lateral and top cubes faces due to the application of HT after the sandblasting post-process. A similar behaviour was observed in the case of the parallelism between each top cube face and the built-up plate for all the analysed stages, as summarized in Table III. In this case, a random distribution was noticed without trends with respect to the cubes location in the plate.

Table III Parallelism of the *XY* cubes faces with respect to built-up plate in the analysed conditions

Condition	XY Parallelism (µm)		
	min	max	mean
AB	42	118	72
SB	40	121	71
SB-HT	39	120	70

Summarizing the results obtained for the geometrical evaluation of the specimen, the location of the cube upon the built-up plate is an important issue to obtain the best flatness value in the case of the top face. This location is not critical in the case of the vertical faces, however, in these cases the sandblasting post-process can strongly improve this geometrical parameter. As it has been noticed, the heat treatment applied after sandblasting practically does not alter flatness. On the other hand, parallelism between top faces of cubes and built-up plate is not modified by sandblasting or heat treatment, which can be explained by the fact that flatness of cubes top faces was only slightly affected by those post-processes.

3.2. Dimensional analysis

Figure 5 shows the deviations of cubes dimensions along the X, Y and Z axes (length, width, and height) with regard to their respective nominal values for all stages of the specimen.

Distributions of these deviations over the plate are quite similar to those in the case of flatness analysed previously and shown in Figure 3, as it is the effect caused by the post-processes upon them.

That is, the dimensional deviation of the cubes is randomly distributed in the case that vertical faces are involved (for the dimensions in the X and Y axes), whereas a trend appears for the height dimension regarding the X and Y location of the cube upon the

plate, where the top surfaces of the cube are involved, which can be related to the compaction roller movement. In relation to post-processes, sandblasting strongly affects the deviation detected for the dimensions that are dependent of cubes vertical faces, i.e. horizontal dimensions (length and width dimensions), without practically altering the deviations observed for the vertical dimensions (height dimension). In this case, heat treatment also does not alter significatively the deviations obtained after SB postprocessing.

Figure 5 Distribution of deviations of the X, Y, Z cubes dimensions upon the built-up plate for all conditions

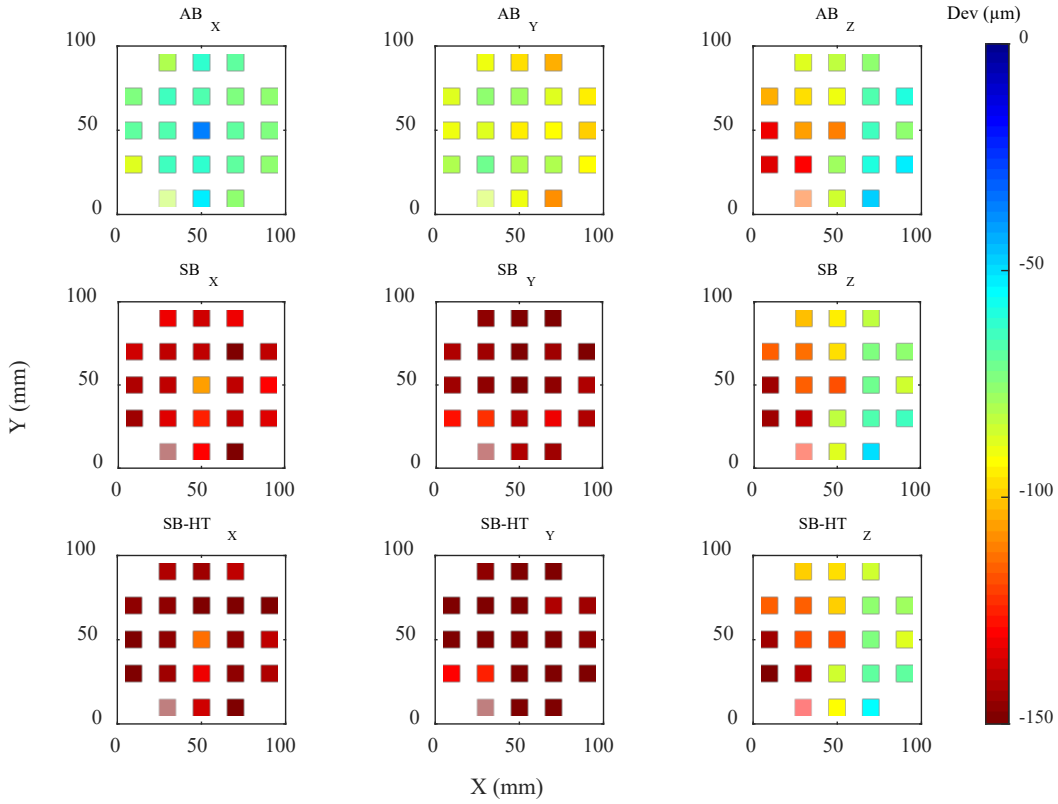

However, it has to be noticed that all of the deviations evaluated in AB condition were negative, as collected in Table IV. This table shows the average value and the standard deviation of the 21 cubes. That means that the actual dimensions of cubes are smaller than their respective nominal values. In this first stage, comparing the deviations detected for the different directions, X, Y and Z, it can be noticed that lower deviations are achieved

in the case that the dimension is aligned to the roller direction movement (X direction) during the powder compaction procedure. At this stage, the average deviation of the X dimension (length) is -69.2 µm, and it reaches -89.4 µm for the Y dimension (width), and -88.7 µm for the Z dimension (height). As it can be seen, the variability reflected by the standard deviation values is consistent with the flatness of the faces involved in the measurement of each dimension. Therefore, a greater variability of about 27 µm appears in height dimensions while it remains below 10 µm in length and width dimensions.

After the sandblasting operation, the dimensions of the cubes are strongly altered due to the elimination of material projections attached to the vertical faces, as occurred with flatness. In fact, although this post-process leads to an improvement in flatness, it produces also an increase in the deviation of the cubes dimensions because the cubes length and width are smaller than before. At this stage (SB), the cubes dimensions deviations are even higher than in AB condition (average deviations of -137.1 µm, -143.4 µm, -97.7 µm in X, Y, Z dimensions, respectively), due to the sandblasting erosion effect. Undoubtedly the effect of flattening the roughness profile (in SLM, there are very high values of Ra) has more effect on the vertical faces than on the horizontal top faces. Figure 6 details this erosion effect by assigning the deviation evolution from AB to SB stages to each cube. Table V summarizes the main values of this evolution. As it can be noticed, this erosion barely affects the vertical dimensions (heights) of the cubes.

Table IV Deviations of cubes dimensions in all the specimen conditions

Condition	Deviation of cubes dimensions (µm)					
	$\overline{X}$	σ_X	$\overline{Y}$	σ_Y	$\overline{Z}$	σ_Z
AB	-69.2	11.0	-89.4	9.2	-88.7	26.1
SB	-137.1	9.9	-143.4	8.1	-97.7	27.5
SB-HT	-144.7	10.0	-149.7	8.7	-100.2	27.1

Figure 6 Sandblasting erosion effect distribution upon the built-up plate

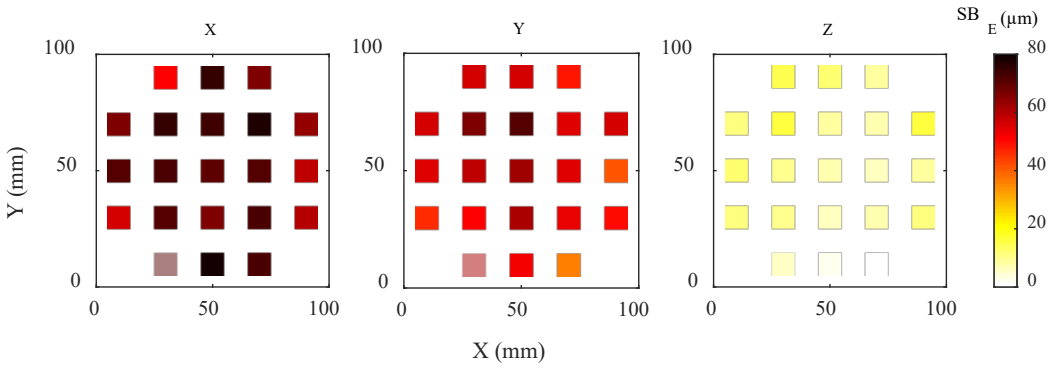

Table V Sandblasting erosion effect in the cubes dimensions

Direction	SB Erosion (µm)		
	min	max	mean
X	51	78	67.9
Y	35	71	54.0
Z	1	16	9.0

In relation with the dimensional analysis of distances between twin faces of different cubes along X and Y directions, Figure 7 shows the deviations detected along the five rows represented in Figure 1a. As it can be noticed, the deviations are negative in AB condition, decrease after the sandblasting post-process (SB condition) and remain practically unaltered by the subsequent heat treatment, (SB-HT condition).

Figure 7 Deviations detected for distances between twin cubes faces along the X axis for the five rows

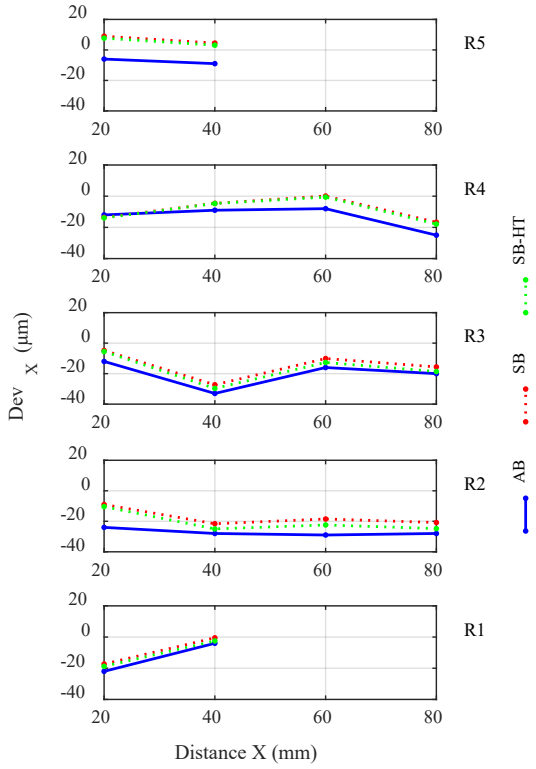

The evaluation of the distance deviation along the five rows is summarized in Table VI. As mentioned above, the sandblasting permits to reduce the mean distance deviation in all rows. Heat treatment post-process practically does not alter these deviations, which are slightly worse than those corresponding to SB condition for rows R1 to R4, and slightly better for row R5. These changes could be related to thermal permanent deformation suffered by the built-up plate during the HT post-process. Nevertheless, the small deformation affecting the distance between faces can be caused by the deformation suffered by the base plate which concentrates much more mass than the mass of the cubes.

Table VI Deviations in distances measurement along the five rows of the specimen

	Row Distance Deviation (µm)									
	R1		**R2**		**R3**		**R4**		**R5**	
Condition	$\overline{Dev_X}$	σ	$\overline{Dev_X}$	σ	$\overline{Dev_X}$	σ	$\overline{Dev_X}$	σ	$\overline{Dev_X}$	σ
AB	-13.0	12.7	-27.3	2.2	-20.3	9.1	-13.5	7.9	-7.5	2.1
SB	-8.9	11.9	-17.5	5.8	-14.5	9.6	-8.7	7.8	6.8	3.2
SB-HT	-10.7	11.5	-20.7	6.9	-16.6	10.2	-9.3	8.0	5.4	3.3

A similar representation, but now for the distances between twin faces along the Y axis (Figure 1a), is shown in Figure 8. In first place, it can be observed that the deviations are generally higher than those measured along the rows. Observing the Figure 8 and the information summarized in Table VII, it can be noticed that the post-processes deviations are worse for almost all the columns. Anyway, all the smaller deviation values could be related to the thermal deformations suffered by the built-up plate commented above.

Figure 8 Deviations detected for distances between twin cubes faces along the Y axis for the five columns

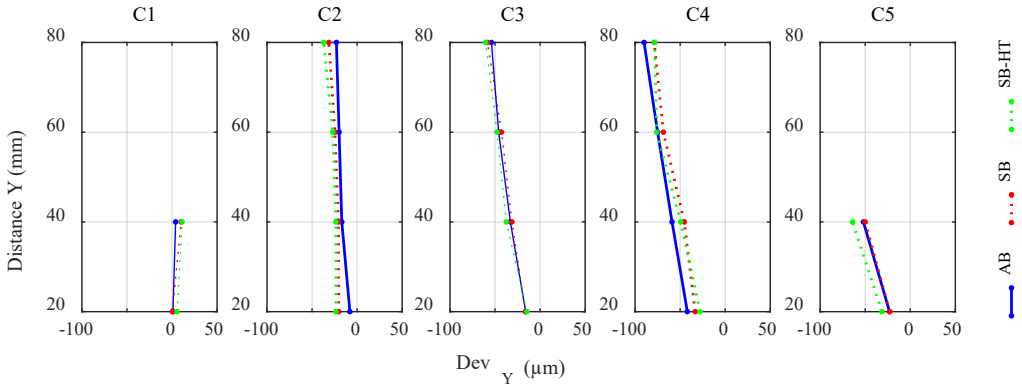

Table VII Deviations in distances measurement along the five columns of the specimen

	Column Distance Deviation (µm)									
	C1		C2		C3		C4		C5	
Condition	$\overline{Dev_Y}$	σ	$\overline{Dev_Y}$	σ	$\overline{Dev_Y}$	σ	$\overline{Dev_Y}$	σ	$\overline{Dev_Y}$	σ
AB	2.5	2.1	-17.0	6.5	-37.3	16.6	-66.5	20.7	-37.5	20.5
SB	5.2	6.8	-24.3	5.1	-37.2	17.8	-56.5	20.9	-36.4	19.2
SB-HT	8.4	4.0	-27.8	6.4	-40.1	19.4	-57.9	24.0	-47.8	23.1

Summarizing the results obtained for the dimensional evaluation of the specimen, in this case it can be stated that, the SLM process produces parts that have smaller dimensions than the nominal ones. This effect depends on the direction of the evaluated dimension of the parts, i.e. X, Y or Z direction, and is differently affected by the sandblasting post-process, being practically unaltered by the HT applied after.

4. Conclusions

In this work the influence of two post-processes of the Selective Laser Melting have been analysed, sandblasting and ulterior stress-relieving heat treatment. Furthermore, the influence of part location upon the built-up plate and related to the machine roller compaction movement are also analysed from the point of view of the geometrical and dimensional accuracy. To achieve this, a specimen consisting of a grid of equally spaced cubes distributed upon the built-up plate was manufactured and measured in different stages, that is, as built condition (AB), after a regular sandblasting (SB) and after a stress relieving heat treatment applied to the previous condition (SB-HT). After each of these conditions, a geometrical and dimensional accuracy analysis of the specimen was carried out. For the geometrical analysis, the flatness of the cubes faces and the parallelism between the top faces and the built-up plate were analysed. On the other hand, in the dimensional analysis, dimensions of the cubes and distances between them related to the machine axes were evaluated.

In case of the geometrical analysis, it was detected that the flatness of top faces (horizontal) was dependant on the location of the cube upon the built-up plate whereas there was no influence on flatness of the lateral planes. These effects can be related to the different compaction capability of the roller in X and Y directions. Moreover, an important improvement of flatness was reached by means of the sandblasting post-process for the lateral faces, i.e., 37.4% for XZ and 35.0% for XY cubes faces. Meanwhile, the sandblasting post-process improvement was only of 3.8% for the top faces. In case of the heat treatment applied after sandblasting, no remarkable changes were observed in the flatness analysis of the specimen. Both sandblasting and heat treatment barely modify the parallelism between the top cubes faces and the built-up plate, showing a random distribution upon the plate in all the analysed conditions.

In the dimensional analysis of cube size, systematic negative deviations were detected for all the cubes dimensions, which are aggravated by the application of sandblasting, but being unaltered by the subsequent heat treatment applied.

Regarding the relative distances between parallel faces of cubes, minor relative distance deviations were observed for the cubes aligned along the X axis of the machine than those aligned along the Y axis, i.e. minor deviations in the roller direction movement. These deviations were slightly improved by the post-processes in the case of the X aligned distances being barely unaltered in case of Y aligned ones.

Based on these results, it is recommended to use sandblasting post-process in order to improve the geometrical quality (flatness and parallelism) of the SLM parts.

The dimensional evaluation of the specimen found smaller dimensions of cubes than the nominal ones. The reduction caused by the sandblasting post-process (erosion ratio) is greater in the case of length (67.9 μm in X direction) and width (54.0 μm in Y direction) than in the height dimension (9.0 μm in Z direction), being practically unaltered by the subsequent heat treatment. Therefore, a direction dependent rescaling is strongly recommended during the design phase to compensate these undesirable size reduction ratios.

On the other hand, analysing the results obtained for distances between different manufactured parts distributed upon the built-up plate, it also has been stated that the dimensions are smaller than nominal ones, having better quality in the case of rows than in columns distances. That is, deviations detected in dimensions parallel to the roller movement are lower. Thus, a distribution of different parts manufactured at the same time and also for large parts along the X direction is recommended. Furthermore, it is recommended to orientate parts aligned with the X axis of the machine, due to smaller dimensional deviations between parts detected in this direction.

In this work it has been noticed that the heat treatment post-process does not produce remarkable changes both in geometrical and dimensional accuracy. However, it should be considered that this treatment has been applied after sandblasting. In case this heat treatment post-process had been applied previously, the sandblasting erosion ratio would be negligible due to the high hardness induced by the heat treatment post-process.

As a future work, the application of a methodology similar to the one presented in this article to SLM tailor-made artefacts has been planned. On other line of the research, there is an unavoidable post-process whose influence has not been sufficiently studied, as is the case of the cutting or separation of parts from the built-up plate. This operation can cause dimensional variations in the parts after separation, due to the release of the residual stresses induced by the AM process or other post-processes.

Acknowledgements

The authors thank to two student grants awarded by the University Institute of Industrial Technology of Asturias (IUTA, ref. SV-18-GIJON-1-06) and by the Young researcher mobility program of SIF (Manufacturing Engineering Spanish Society). And also, to the financial support provided by the Spanish Ministry of Science, Innovation and Universities (project DPI2017-89840-R, through FEDER-ERDF funds) and by the Junta de Castilla y León (project LE027P17-FEDER funds).

References

3DSystems (2017), “Direct Metal Printers Metal Additive Manufacturing with the ProX DMP 3D printers”

AlMangour, B. and Yang, J. M. (2016), "Improving the surface quality and mechanical properties by shot-peening of 17-4 stainless steel fabricated by additive manufacturing", *Materials & Design*, Vol. 110, pp. 914-924.

Avanzini, A., Battini, D., Gelfi, M., Girelli, L., Petrogalli, C., Pola, A. and Tocci, M. (2019), "Investigation on fatigue strength of sand-blasted DMLS-AlSi10Mg alloy", *Procedia Structural Integrity*, Vol. 18, pp. 119-128.

Bagehorn, S., Mertens, T., Greitemeier, D., Carton, L. and Schoberth, A. (2015), "Surface finishing of additive manufactured Ti-6Al-4V - a comparison of electrochemical and mechanical treatments", in *Proceedings of European Conference for Aeronautics and Space Sciences (EUCASS 2015) in Kraków, Poland, 2015*.

Bagherifard, S., Beretta, N., Monti, S., Riccio, M., Bandini, M. and Guagliano, M. (2018), "On the fatigue strength enhancement of additive manufactured AlSi10Mg parts by mechanical and thermal post-processing", *Materials & Design*, Vol. 145, pp. 28-41.

Bai, Y., Zhao, C., Yang, J., Ying Hsi Fuh, J., Feng Lu, W., Weng, C. and Wang, H. (2020), "Dry mechanical-electrochemical polishing of selective laser melted 316L stainless steel", *Materials & Design*, (In Press, Journal Pre-proof https://doi.org/10.1016/j.matdes.2020.108840)

Bartlett, J.L. and Li, X. (2019), "An overview of residual stresses in metal powder bed fusion", *Additive Manufacturing*, Vol. 27, pp. 131-149.

Basha, S.M., Bhuyan, M., Basha, M.M., Venkaiah, N. and Sankar, M.R. (2020), "Laser polishing of 3D printed metallic components: A review on surface integrity", *Materials today: Proceedings*, (In Press, Corrected Proof, https://doi.org/10.1016/j.matpr.2020.02.443)

Cheng, B., Shrestha, S. and Chou, K. (2016), "Stress and deformation evaluations of scanning strategy effect in selective laser melting", *Additive Manufacturing*, Vol. 12, pp. 240-251.

Cuesta, E., Gesto, A., Álvarez, B.J., Martínez-Pellitero, S., Zapico, P. and Giganto, S. (2019), "Dimensional accuracy analysis of Direct Metal Printing machine focusing on roller positioning errors", *Procedia Manufacturing*. Vol. 41, pp. 2-9.

Das, P., Chandran, R., Samant, R. and Anand, S. (2015), "Optimum Part Build Orientation in Additive Manufacturing for Minimizing Part Errors and Support Structures", *Procedia Manufacturing*, Vol. 1, pp. 343-354.

Gale, J. and Achuhan, A. (2017), "Application of ultrasonic peening during DMLS production of 316L stainless steel and its effect on material behaviour", *Rapid Prototyping Journal*, Vol. 23 (6), pp. 1185-1194.

Giganto, S., Zapico, P., Castro-Sastre, M.A., Martínez-Pellitero, S., Leo, P. and Perulli, P. (2019), "Influence of the scanning strategy parameters upon the quality of the SLM parts", *Procedia Manufacturing*. Vol. 41, pp. 698-705.

Ginestra, P., Ceretti, E., Lobo, D., Lowther, M., Cruchley, S., Kuehne, S., Villapun, V., Cox, S., Grover, L., Shepherd, D., Attallah, M., Addison, O. and Webber, M. (2020), "Post Processing of 3D Printed Metal Scaffolds: a Preliminary Study of Antimicrobial Efficiency", *Procedia Manufacturing*, Vol. 47, pp. 1106-1112.

Hackel, L., Rankin, J. R., Rubenchik, A., King, W. E. and Matthews, M. (2018), "Laser peening: A tool for additive manufacturing post-processing", *Additive Manufacturing*, Vol. 24, pp. 67-75.

Han, S., Salvatore, F., Rech, J. and Bajolet, J. (2020), "Abrasive flow machining (AFM) finishing of conformal cooling channels created by selective laser melting (SLM)", *Precision Engineering*, Vol. 64, pp. 20-33.

ISO 10360-2 (2009), “Geometrical product specifications (GPS) - Acceptance and verification tests for coordinate measuring machines (CMM) - CMMs used for measuring linear dimensions”, *International Organization for Standardization*, Geneva, Switzerland.

Kalms, M., Narita, R., Thomy, C., Vollertsen, F. and Bergmann, R.B. (2019), “New approach to evaluate 3D laser printed parts in powder bed fusion-based additive manufacturing in-line within closed space”, *Additive Manufacturing*, Vol. 26, pp. 161-165.

Kaplanskii, Y.Y., Sentyurina, Z.A., Loginov, P.A., Levashov, E.A., Korotitskiy, A.V., Travyanov, A.Y. and Petrovskii, P.V. (2019), “Microstructure and mechanical properties of the (Fe,Ni)Al-based alloy produced by SLM and HIP of spherical composite powder”, *Materials Science and Engineering: A*, Vol. 743, pp. 567-580.

Koutiri, I., Pessard, E., Peyre, P., Amlou, O. and De Terris, T. (2018), “Influence of SLM process parameters on the surface finish, porosity rate and fatigue behavior of as-built Inconel 625 parts”, *Journal of Materials Processing Technology*, Vol. 255, pp. 536-546.

Lesyk, D.A., Martinez, S., Mordyuk, B.N., Dzhemelinskyi, V.V., Lamikiz, A. and Prokopenko, G.I. (2020), “Post-processing of the Inconel 718 alloy parts fabricated by selective laser melting: Effects of mechanical surface treatments on surface topography, porosity, hardness and residual stress”, *Surface and Coatings Technology*, Vol. 381, pp. 125136:1-16.

Liu, S. and Guo, H. (2020) “Influence of hot isostatic pressing (HIP) on mechanical properties of magnesium alloy produced by selective laser melting (SLM)”, *Materials Letters*, Vol. 265, pp. 127463.

Matsumoto, M., Shiomi, M., Osakada, K. and Abe, F. (2002), “Finite element analysis of single layer forming on metallic powder bed in rapid prototyping by selective laser processing”, *International Journal of Machine Tools and Manufacture*, Vol. 42(1), pp. 61-67.

Morton, W., Green, S., Rennie, A. E. W. and Abram, T. N. (2012), “Surface finishing techniques for SLM manufactured stainless steel 316L components”, in *Proceedings of 5th International Conference on Advanced Research and Rapid Prototyping in Leiria, Portugal, 2012,* pp. 503-509.

Mostafa, A., Picazo Rubio, I., Brailovski, V., Jahazi, M. and Medraj, M. (2017), “Structure, texture and phases in 3D printed IN718 alloy subjected to homogenization and HIP treatments”, *Metals*, Vol. 7(6), pp. 196.

Mower, T.M. and Long, M.J. (2016), “Mechanical behavior of additive manufactured, powder-bed laser-fused materials”, *Materials Science and Engineering: A*, Vol. 651, pp. 198-213.

Senin, N., Thompson, A. and Leach, R.K. (2017), “Characterisation of the topography of metal additive surface features with different measurement technologies”, *Measurement Science and Technology*, Vol. 28 No. 9, pp. 095003:1-12.

Townsend, A., Racasan, R. and Blunt, L. (2018), “Surface-specific additive manufacturing test artefacts”, *Surface Topography: Metrology and Properties*, Vol. 6 No. 2, pp. 024007:1-10.

Tilita, G. A., Chen, W., Leung, C. K., Kwan, C. C., Ma, R. L. and Yuen, M. M. (2017), “Influence of ultrasonic excitation on the mechanical characteristics of SLM 304L stainless steel”, *Procedia engineering*, Vol. 216, pp. 18-27.

Van Elsen, M., Al-Bender, F. and Kruth, J. (2008), "Application of dimensional analysis to selective laser melting", *Rapid Prototyping Journal*, Vol. 14 No. 1, pp. 15-22.

Yang, Y., Lu, J., Luo, Z. and Wang, D. (2012), "Accuracy and density optimization in directly fabricating customized orthodontic production by selective laser melting", *Rapid Prototyping Journal*, Vol. 18 No. 6, pp. 482-489.

Wang, Z., Xiao, Z., Huang, C., Wen, L. and Zhang, W. (2017), "Influence of ultrasonic surface rolling on microstructure and wear behavior of selective laser melted Ti-6Al-4V alloy", *Materials*, Vol. 10(10), pp. 1203.

Zhang, H., Gu, D., Ma, C., Guo, M., Yang, J. and Wang, R. (2019), "Effect of post heat treatment on microstructure and mechanical properties of Ni-based composites by selective laser melting", *Materials Science and Engineering: A*, Vol. 765, pp. 138294.

Zapico, P., Giganto, S., Martínez-Pellitero, S., Fernández-Abia, A.I. and Castro-Sastre, M.A. (2018), "Influence of Laser Energy in the Surface Quality of Parts Manufactured by Selective Laser Melting", in *Proceedings of DAAAM International Symposium on Intelligent Manufacturing and Automation in Zadar, Croatia, 2018*, DAAAM International, Vienna, pp. 0279-0286.